Aided Self-Assembly of Porphyrin Nanoaggregates into Ring-Shaped Architectures

Marga C. Lensen,[a] Ken Takazawa,[b, c] Johannes A. A. W. Elemans,[a] Cecile R. L. P. N. Jeukens,[b] Peter C. M. Christianen,*[b] Jan C. Maan,[b] Alan E. Rowan,*[a] and Roeland J. M. Nolte[a]

Abstract: The formation of micrometer-sized, highly ordered porphyrin rings on surfaces has been investigated. The porphyrin-based nanoarchitectures are formed by deposition from evaporating solutions through a surface dewetting process which can be tuned by variations in the substitution pattern of the molecules used, the coating of the surface and the conditions under which the evaporation takes place. Control over the combined self-assembly and surface dewetting results in nanorings possessing a defined internal architecture. The ordering of the molecules within the rings has been studied by a variety of microscopy techniques (TEM, AFM, fluorescence microscopy) and the exact ordering of the porphyrins within the rings has been quantified.

Keywords: fluorescence · nanostructures · porphyrinoids · self-assembly · surface chemistry

Introduction

The design and construction of multi-chromophoric arrays is currently a topic of great interest. Circular porphyrin arrays are of particular interest because of their resemblance to the light-harvesting complexes (LH1 and LH2) of the natural photosynthetic system.[1–3] In these pigment–protein complexes the constituting porphyrins are arranged in a precise orientation in which the energy gradient is ideal for its light-harvesting function. In many functional architectures in nature, the complex superstructure is the result of the self-assembly and self-organization of the smaller building blocks.[4] Since the advent of supramolecular chemistry, chemists have been attempting to fabricate functional devices from simple molecular components that are programmed to self-organize into hierarchical structures, in an analogous fashion to biological systems.[5] To succeed in this goal, it is very important to have control over the self-organization process at different hierarchical levels. First, the constituting molecules with desired (photo)catalytic, electronic, magnetic or optical properties must be equipped with handles for intermolecular recognition.[6,7] Second, the building blocks need to self-assemble into larger structures with a predictable morphology. Third, it is a challenge to control the self-organization of these, often discrete, self-assembled supermolecules into functional nanoarchitectures. As a last step, the collection of these structures should result in a functional device or material.[8,9]

In this paper the fabrication of micrometer-sized porphyrin rings with pronounced polarized optical properties is described. The formation of these ordered circular porphyrin structures is governed by tandem self-assembly processes and constitutes a further step towards the construction of functional nanoscale architectures in the field of catalysis and molecular electronics. In view of potential optical applications, it is of particular importance to control the desired arrangement of the porphyrins with respect to each other since the communication between chromophores depends heavily on their relative orientation.[10] In recent years, the accessibility and resolution of optical and mechanical techniques on the nanometer scale has increased to an extent that

[a] M. C. Lensen, Dr. J. A. A. W. Elemans, Dr. A. E. Rowan, Prof. R. J. M. Nolte
Department of Organic Chemistry, NSRIM Center
University of Nijmegen
Toernooiveld 1, 6525 ED, Nijmegen (The Netherlands)
Fax: (+31) 24-3652929
E-mail: rowan@sci.kun.nl

[b] Dr. K. Takazawa, C. R. L. P. N. Jeukens, Dr. P. C. M. Christianen, Prof. J. C. Maan
High Field Magnet Laboratory, NSRIM Center
University of Nijmegen
Toernooiveld 7, 6525 ED Nijmegen (The Netherlands)
Fax: (+31) 24-3652440
E-mail: peterc@sci.kun.nl

[c] Dr. K. Takazawa
Tsukuba Magnet Laboratory
National Institute for Materials Science
3-13 Sakura, Tsukuba, 305-0003 (Japan)

 DOI: 10.1002/chem.200305436

single chromophoric units can be characterized.[11–13] Detailed studies of the ring-shaped porphyrin assemblies using these techniques will lead to a fundamental understanding on their internal structure, the exciton coupling between the chromophores and hence the possibility to construct nanosized rings that can mimic the natural LH2 systems and transfer excitation energy within the ring.

As part of our efforts to construct functional architectures, we have synthesized oligomeric porphyrin arrays **1** and **2** (Figure 1), which can form large rings on solid substrates as we have previously reported[14] and are able to form stable π-stacked columnar arrays at an air–water interface.[15] The extended π-surface in combination with their disk-like shape makes them self-assemble in solution into columnar stacks. In addition, the alkyl tails provide the molecular aggregates with affinity to adsorb on a carbon surface.[16] In the case of hexamer **1a**, the formation of long columnar stacks was directly observed by scanning tunneling microscopy (STM) at a solution–graphite interface.[17] Hexamer **1b** was designed to aggregate more strongly than **1a** due to stronger π–π interactions,[18] whilst hexamer **2** was investigated to study a nonlinear optical behavior effect that might be expected to result from the chirality of the molecule.

The formation of the ring-shaped architectures is related to the physical processes of dewetting, surface tension and solvent and solute dynamics.[19–21] Consequently this phenomenon is not restricted to porphyrins but can be applied to other materials as well.[22,23] It has for example been shown that rings can be formed from inorganic colloidal particles.[24–28]

There are two distinct mechanisms which describe ring-formation processes, the "coffee-stain mechanism" and the "pinhole mechanism" (Figure 2). The coffee-stain mechanism, which was introduced and later elaborated by Deegan,[29,30] explains the formation of ring-like stains from solution droplets. During evaporation of the solvent the solute is concentrated at the perimeter of the droplet provided that the contact line of the solution with the solid substrate is pinned. To compensate for the evaporative losses, an outward flow of fluid carries the dispersed material from the interior to the edge of the drop and deposits it as a solid ring. If the solute is not transferred completely, a fraction of the material remains inside the resulting ring. In the case of porphyrin rings formed by **1** and **2** it is observed that there

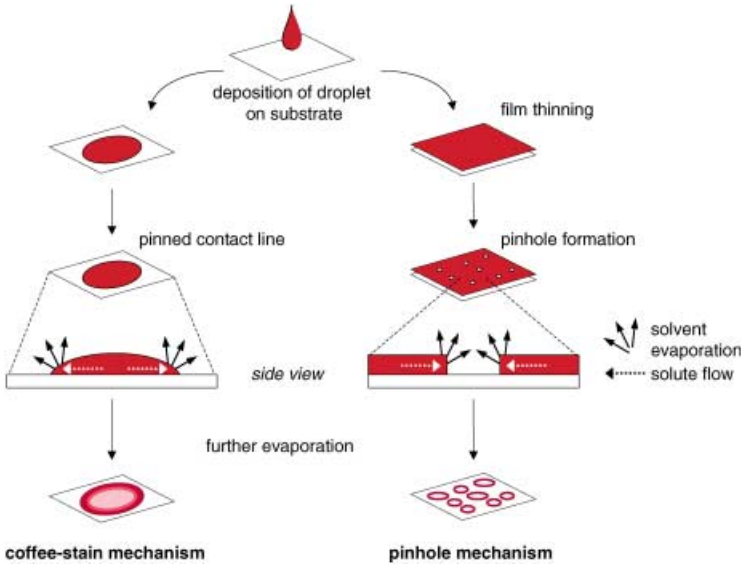

Figure 2. Schematic representation of the ring-formation process according to the coffee-stain mechanism (left) and the pinhole mechanism (right).

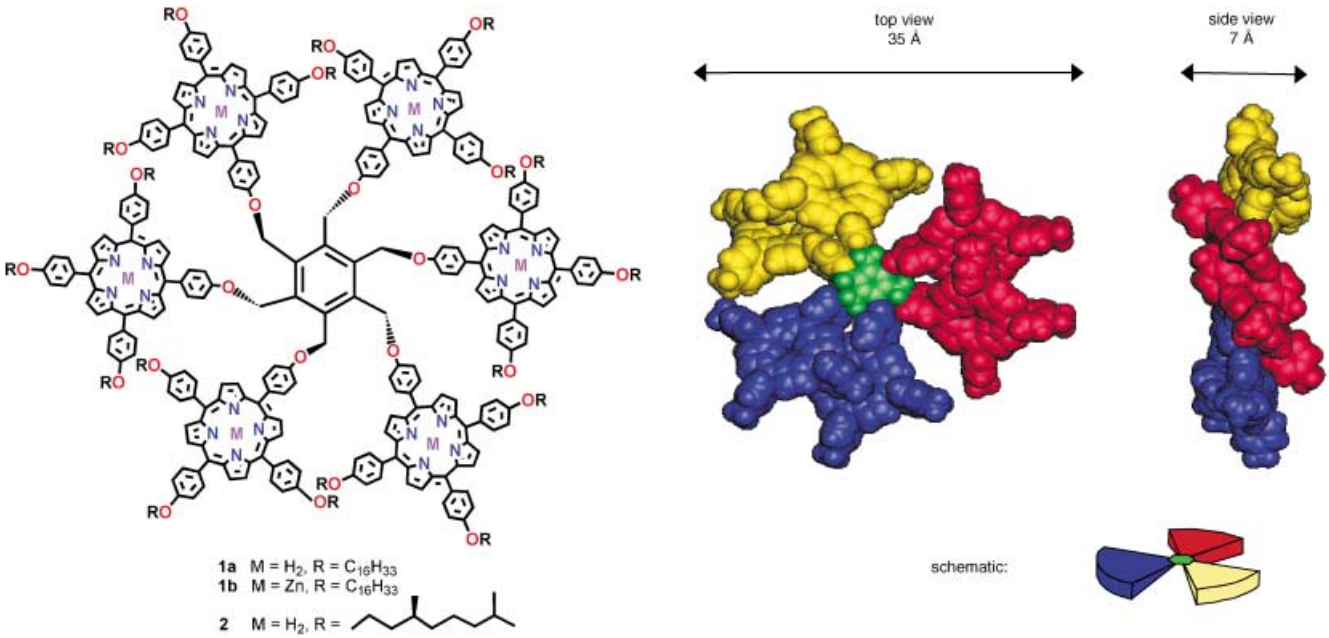

Figure 1. Hexa-porphyrin molecules **1** and **2** and their proposed 3D structure in solution as was determined from ^{1}H NMR measurements. Alkyl tails have been omitted for clarity.

is no detectable fluorescence coming from the inside of the rings (see below). This indicates that the mechanism by which these porphyrin rings are formed is different from that of the coffee-stain mechanism. It is proposed that in this case a so-called pinhole mechanism occurs in which the formation of holes in the thinning liquid films account for the ring-formation.[28,31,32]

Upon evaporation of a solution film on a wetted substrate, the film thins to a thickness at which holes nucleate. At this equilibrium thickness there is a balance between thinning (by evaporation) and wetting of the surface. The holes open while the self-assembling particles are collected in the growing inner perimeter. The spherical nucleation sites grow in size while the evaporation continues and the solution becomes more and more concentrated. The evaporation speed is higher at the edge of the pinhole than in the bulk of the solution film.[29,30,33] To compensate for this loss of liquid, an inward flow of solute occurs, resulting in a further concentration at the inner edge of the ring structure. This process continues until the solvent has evaporated completely and the collected material is deposited as rings. According to this mechanism, material can be found on the outside of the rings, which is for **1** and **2** indeed the case when very concentrated solutions are applied.[20]

The rupture of the solution film is due to surface instability and can occur via two possible mechanisms, by dewetting at heterogeneous nucleation sites and by spinodal dewetting.[34–36] Heterogeneously nucleated holes form at the early stage during evaporating and can grow continuously. As a result, the rings are randomly distributed over the sample and will have different diameters. On homogeneous surfaces, spinodal dewetting can occur, generally at a later stage where the film is thinner. In this case the dewetting is due to surface undulations with a periodicity that is correlated to the spinodal length scale and can be derived from linear analysis.[37–39] The rings formed via this mechanism are expected to be smaller in diameter, more monodisperse in size and are found at a certain mean distance.

The porphyrin rings have been investigated before by a variety of techniques such as confocal fluorescence microscopy (CFM), atomic force microscopy (AFM) and near-field scanning optical microscopy (NSOM). Initial studies have suggested that the porphyrin molecules are randomly oriented within the rings.[14,40,41] Annealing of the rings allowed the molecules to order to some extent, however, the precise ordering within the rings has not yet been determined. In order to achieve complete understanding of the ring-formation process and of the ordering within the rings more extensive combined microscopy and spectroscopy studies have been carried out. The different dewetting mechanisms that play a role during the ring-formation process will be discussed and correlated to ring sizes and internal order. Moreover, the ordering on a molecular scale will be quantified in addition to the microscopic ordering throughout the ring structures. Finally, this report will demonstrate that we can achieve control of these supramolecular architectures on different levels in the formation process, resulting in control over size and shape of the rings and their internal ordering.

Results

The porphyrin rings were prepared by depositing a droplet of a porphyrin hexamer solution in chloroform on a solid substrate and allowing the solvent to evaporate. Figure 3 shows a typical AFM image of porphyrin rings on a hydrophilic, carbon-coated glass substrate (a) together with the cross-section through a representative ring (b), which shows that the rim of this ring, which is 2 μm in diameter, is 15 nm high and 0.2 μm wide. Analysis of many (60) rings on a typical area of the sample revealed that the rings were on an average 1.4 μm in diameter (Figure 3c), all had a typical thickness of 200 nm and were 15–20 nm high.

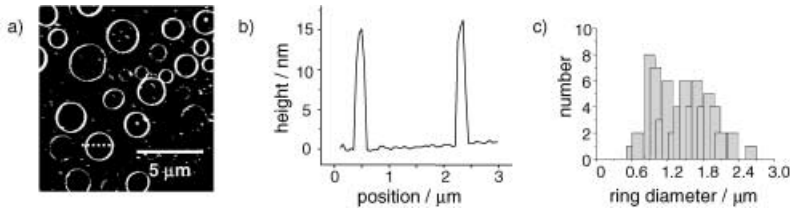

Figure 3. a) AFM image of rings of hexa-porphyrin **1a** on hydrophilic carbon-coated glass. b) Cross section along the dotted line in a). c) Number of rings with diameters as measured by AFM.

Samples of rings formed from hexamers **1** and **2** were prepared on four different substrates at room temperature and analyzed by fluorescence microscopy. Table 1 summarizes

Table 1. Ring sizes and polarization effects as observed by fluorescence microscopy for rings formed on various substrates.

Molecule	Substrate	Ring size [μm]	Polarized fluorescence
	hydrophobic carbon-coated grid	1–20	no[a]
	untreated glass	no rings[b]	–
1	hydrophobic carbon-coated glass	2–20	no
	hydrophilic carbon-coated glass	1–4	strong
	hydrophobic carbon-coated grid	1–20	weak[c]
	untreated glass	no rings[b]	–
2	hydrophobic carbon-coated glass	1–5	weak
	hydrophilic carbon-coated glass	1–4	strong

[a] After annealing the sample for 48 h at 90 °C, rings smaller than 5 μm were observed to possess weakly polarized emission. [b] Ill-defined ring-shaped aggregates were observed. [c] Only rings smaller than 5 μm were observed to give weakly polarized emission.

the ring size distributions and the occurrence of polarization effects (see below) within the rings.

In order to investigate the influence of the surface on the ring-formation process, in Figure 4 the real-space fluorescence microscopy images of ring samples of **1a** on a (hydrophobic) carbon-coated copper grid (a), untreated glass (b), hydrophobic carbon-coated glass (c), and hydrophilic carbon-coated glass (d) are compared.

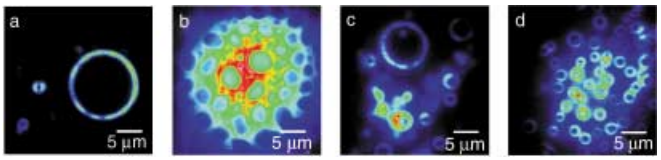

Figure 4. Fluorescence images (false colors) of rings formed from **1a** on various substrates prepared under ambient conditions on a) (hydrophobic) carbon-coated copper grid, b) untreated glass, c) hydrophobic carbon-coated glass, and d) hydrophilic carbon-coated glass.

The rings formed by **1a** were similar to those observed before.[14] The size, the distribution of ring sizes and the number of rings formed in a certain area was strongly dependent on the substrate used, which indicates that the surface characteristics considerably influence the ring-formation process. The rings on the hydrophilic carbon-coated glass were observed to have a highly monodisperse size distribution (Figure 4d). The fluorescence microscopy images of the rings formed from hexamer **1b** did not differ significantly from those formed from **1a** and also molecules of hexamer **2** formed well-defined rings on carbon-coated copper grids and on hydrophobic or hydrophilic carbon-coated glass (images not shown).

The fluorescence microscopy of the rings using polarized excitation light and polarized detection of the emission revealed that only the small rings (up to 5 µm) of **1a** and **2** showed fluorescence anisotropy. The polarized fluorescence microscopy images of the rings of **1a** on hydrophilic carbon-coated glass are depicted in Figure 5. When the excitation and the detection polarization are both oriented vertically (Figure 5a), the left and right parts of the rings display higher fluorescence intensity than the upper and lower parts, respectively. Turning both the excitation and the detection polarization 90° (Figure 5b) results in higher fluorescence intensity of the upper and lower parts of the rings. The expression of polarization is directly related to the molecular ordering and the observation of these strong polarization effects indicates that the molecules within a ring are ordered. On this hydrophilic carbon-coated glass substrate, no additional annealing was needed as was reported to be necessary on glass surfaces.[40] The fluorescence microscopy images were also recorded with orthogonally polarized excitation and detection (Figure 5c and d), which resulted in a >80% reduction of the overall fluorescence intensity of the rings.

The degree of polarization can be easily assessed qualitatively from the polarized fluorescence images as shown in Figure 5. Since we propose that the degree of internal order is correlated to the contrast of the fluorescence anisotropy

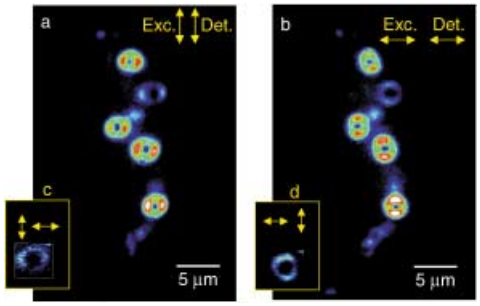

Figure 5. Polarized fluorescence microscopy images of **1a** on hydrophilic carbon-coated glass. Arrows indicate the direction of the excitation and detection polarization.

throughout the rings we evaluated the fluorescence intensity of the rings of **1a** and **2** on hydrophilic carbon-coated glass as a function of the center angle ϕ (Figure 6).

The curves clearly show the modulations with a period of 180°, reflecting the distinct orientations of the transition dipole moments at different segments of the ring. However, the fluorescence intensities at their minima are not zero but have a considerably higher value in rings of both **1a** and **2**. Similar findings were reported for a different supramolecular system.[42] To investigate whether excitation energy is transported within a ring, a fluorescence image was record-

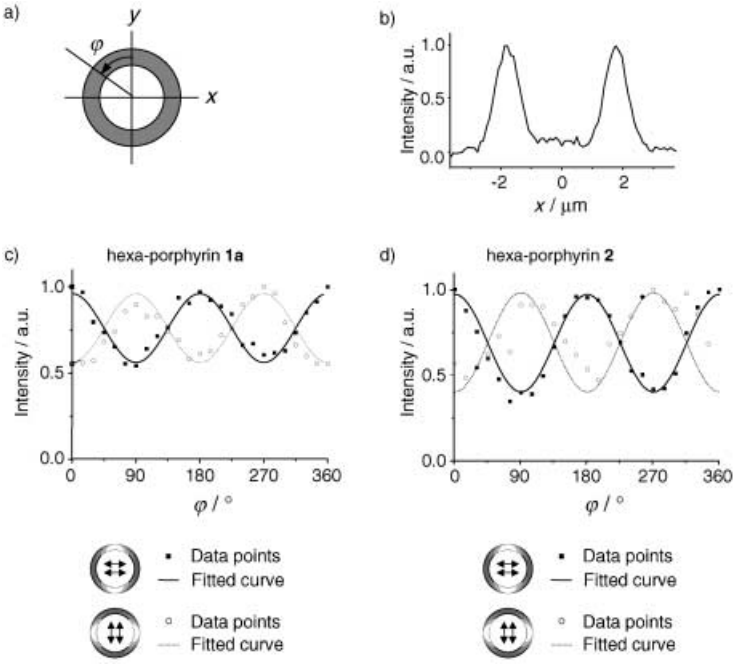

Figure 6. a) Definition of axes and angle ϕ. b) Normalized fluorescence intensity of a ring of hexa-porphyrin **1a** along the x axis. c), d) Normalized fluorescence intensity as a function of the angle ϕ through the rings of **1a** and **2**, respectively. Solid points represent the fluorescence intensity at different positions in the ring as measured with horizontal excitation and detection polarization. Solid lines are curves fitted to the solid data points by a cosine function with a period of 180°. Open points represent the fluorescence intensity at different positions in the ring as measured with vertical excitation and detection polarization. Dashed lines are curves fitted to the open data points by a cosine function with a period of 180°.

ed by exciting the ring by a laser tightly focused down to the diffraction limit (~1 μm in diameter). However, although fluorescence was observed from a slightly larger area than the laser spot, this observation indicates that energy transport in the ring is minimal and not efficient enough to cause the considerable fluorescence intensity at the minima. Therefore, it is more likely that the fluorescence at the intensity minima is due to the conformation of the porphyrin hexamer molecules as represented in Figure 1. Although the hexamers are proposed to be oriented tangentially to the ring, the six individual porphyrin moieties within the molecules are tilted at a slight displacement angle with respect to the central benzene core. The transition dipole moments of absorption and emission are assumed to be both in the porphyrin plane.[10] As a result, at every instance there is a vector component of the transition dipole moment in the polarization direction. Apart from this fundamental argument, it is also not realistic to assume that all molecules are perfectly oriented; there will always be defects in the self-assembled structures.

To evaluate the degree of order of molecules quantitatively, the ordering parameter D was defined as follows:

$$D = |(I_{=} - I_{\parallel} / I_{=} + I_{\parallel})|$$

where $I_{=}$ is the fluorescence intensity at $\phi = 0$, 90, 180 or 270° (Figure 6c and d) measured with horizontal excitation and detection polarization and $I_{\parallel}$ is the intensity measured with vertical excitation and detection polarization, respectively. At every position the measured fluorescence intensity originates from many chromophores with varying orientations with respect to the tangent of the ring. When α is defined as the displacement angle of the dipole moment with respect to the tangential orientation and n is the number of dipole moments that contribute to the fluorescence intensity, $I_{=}$ and $I_{\parallel}$ satisfy the following relations:

$$I_{=} \propto \sum_{n} |M \cos\alpha_{n}|^2$$

$$I_{\parallel} \propto \sum_{n} |M \sin\alpha_{n}|^2$$

where M is the transition dipole moment. Using these relations, D can be expressed as:

$$D = \sum_{n} |\cos^2 \alpha_{n} - \sin^2 \alpha_{n}| / n = \sum_{n} |\cos 2\alpha_{n}| / n$$

This equation implies that D is an average of $|\cos 2\alpha|$. Therefore, $D = 1$ when all dipole moments are oriented tangentially and $D = 0$ when the dipole moments are randomly oriented. Thus, D is appropriate to indicate the degree of order of the molecules. The fit yields $D = 0.26 \pm 0.087$ for rings formed from **1a** (Figure 6c) and $D = 0.41 \pm 0.050$ for rings of **2** (Figure 6d), indicating that the molecules of **2** are ordered slightly better within the rings than the molecules of **1a**.

In order to determine the precise arrangement of molecules of **1a** and **2** within the rings, the optical properties of the rings were further characterized. The absorption spectrum of rings of **1a** is shown in Figure 7a together with the spectrum of a solution of **1a** in chloroform. Since the diameter of the illumination spot was 4 mm, approximately 500 rings contributed to the spectrum. The spectra show the characteristic features of porphyrins, the Soret band at 432 nm and the Q-bands between 500 nm and 700 nm.[10]

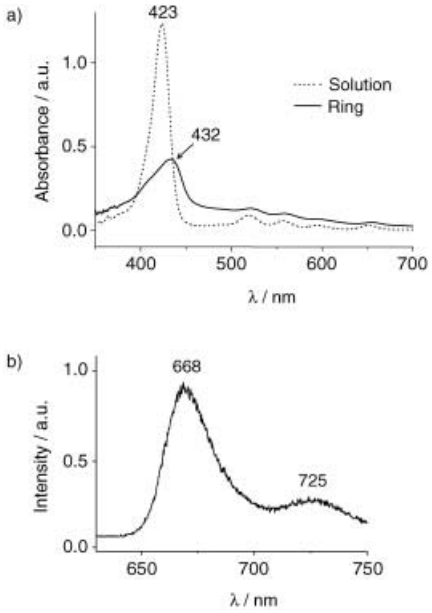

Figure 7. a) Absorption spectra of a chloroform solution of **1a** (3×10^{-7} M; •••••) and of a ring (——) of **1a** on a hydrophilic, carbon-coated glass surface. b) Fluorescence spectrum of a single ring of **1a** on hydrophilic carbon-coated glass.

The spectroscopic features of the porphyrin rings are different from those in solution. Since there are many chromophores that can interact, it is quite complicated to determine which changes should be addressed to excitonic interactions between chromophores within the molecules (intramolecular) or within aggregates (intermolecular).[43,44] The spectral changes include a red-shifted component in the Soret band from solution (423 nm) to the ring (432 nm) indicative of interactions between the porphyrins in a head-to-tail arrangement. This arrangement applies to the overall orientation of the porphyrin moieties within the molecular aggregates but probably also within each hexamer molecule. Thus, we propose that the hexamers aggregate into columnar stacks in which the hexamers are slightly rotated with respect to the neighboring hexamer, as was evidenced by the helicity of the columnar aggregates of chiral hexamer **2**.[45]

Spatially resolved fluorescence spectroscopy was performed to measure the fluorescence spectrum of a single ring on hydrophilic carbon-coated glass. Figure 7b shows the fluorescence spectrum of the upper part of the ring of **1a** measured with horizontally polarized excitation and detection. After excitation of the Soret band at 432 nm, the fluorescence spectrum displays two bands at 668 and 725 nm, re-

spectively. The fluorescence spectrum of the left part of the same ring was recorded with vertical excitation and detection polarization and appeared to be identical to that of the upper part of the ring.

Discussion

Ordering of porphyrin hexamers within the rings: After combining the information from all microscopy and spectroscopy experiments, the precise internal ordering of the molecules in the rings can be derived. We propose that the porphyrin hexamers aggregate in solution into columnar stacks (Figure 8c), which are eventually aligned by the action of dewetting and the consequent solution flow. Once the solvent has completely evaporated, the columnar stacks are deposited around the pinholes as is depicted in Figure 8d. In the following section, the experimental evidence that support this hypothesis will be discussed.

The observed fluorescence intensity reduction over the rings with orthogonally directed excitation and detection (Figure 5c and d) indicates that in the molecules the transition dipole moments of both absorption and emission are oriented parallel with respect to each other. In addition, from the polarized fluorescence images (Figure 5a and b) it can be derived that the transition dipole moments of the molecules must be oriented tangentially to the ring (Figure 8a), in contrast to what has been concluded before.[14]

In Figure 8b the spectroscopic changes that can be expected due to interactions between chromophores are depicted. The red-shifted component in the absorption spectrum of a ring of **1a** as compared to the solution spectrum (Figure 7a) supports the observation that the porphyrin hexamers self-assemble into columnar stacks in a preferred head-to-tail arrangement (Figure 8c). Based on the orientation of the transition dipoles of the molecules, we propose that the stacks are oriented parallel to the radius of the rings (Figure 8d). The cross-section taken from the AFM image (Figure 3b) shows that a typical ring is about 15 nm high. Taking into account the dimensions of the molecules (Figure 1) including the alkyl tails, each columnar aggregate is up to 7 nm in diameter if the tails are fully stretched. This implies that, in order to match the 15 nm height the rings must be built up from no more than three or four aggregates assuming that they are arranged in a hexagonal packing. Likewise, the width of the ring is supposedly related to the length of the columnar stacks. A typical value of 200 nm for a ring of 2 to 5 μm in diameter (as measured by AFM and TEM) corresponds to a stack of about 300 molecules. The individual columnar stacks could not be resolved by AFM but were directly observed by STM.[17]

Factors determining the formation of rings: According to the pinhole mechanism, the ring formation is influenced by the properties of both the solvent and the substrate and together they determine the dewetting process. The ease by which the solution flow carries the molecular aggregates to the inner edge of the growing hole (see Figure 2) is determined by the specific interaction between solvent and substrate. Chloroform is an apolar solvent and is well capable of wetting a hydrophobic (carbon-coated) surface. Also the hydrophilic carbon-coated glass substrate is expected to be wetted by the chloroform solution, but to a lesser extent. Dewetting of the solution films occurs at heterogeneous nucleation sites and via spinodal dewetting when the film is sufficiently thin[23,34,46] and the material is deposited at the edges of the growing holes during the dewetting process.

However, besides dewetting also the simultaneous aggregation processes in solution play an important role in the formation of these rings. The thermodynamically controlled process of intermolecular self-assembly and the rearrangement of the individual molecules within the molecular aggregates in solu-

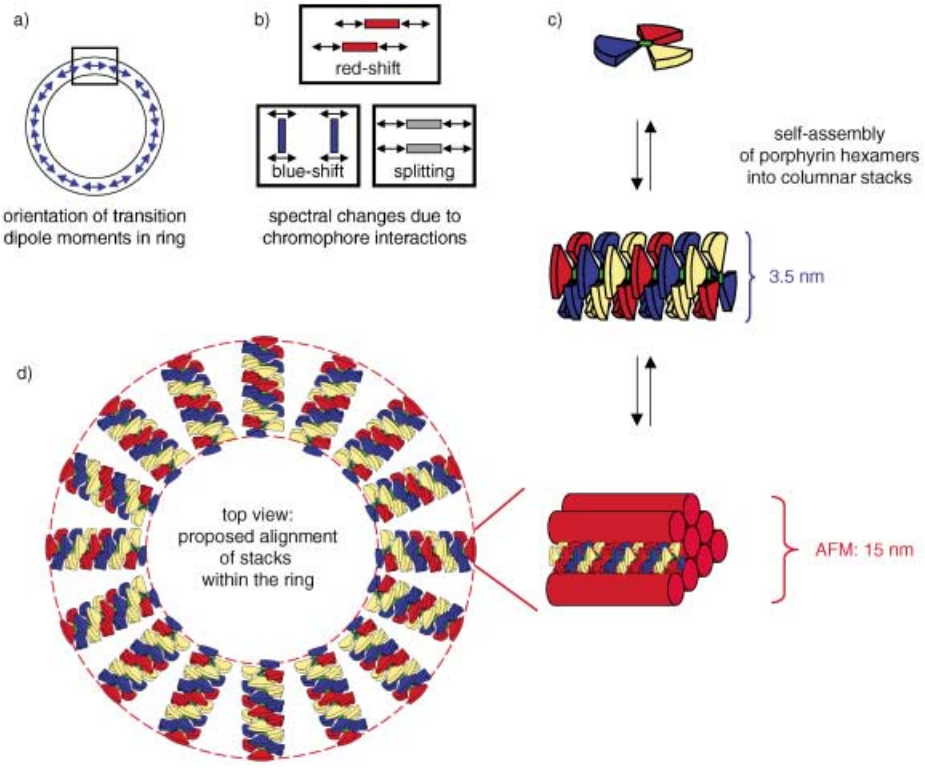

Figure 8. a) Orientation of transition dipole moments of absorption and emission within the ring. b) Schematic diagram of the chromophore interactions and the corresponding spectral changes in the absorption spectrum. c) Schematic representation of a hexamer molecule and molecular orientation of these hexamers in columnar stacks. d) Proposed alignment of columnar stacks within the ring.

tion competes with the kinetically favored adsorption to the surface. These tandem processes depend on the molecular properties (solubility, stackability and adsorption) and the surface characteristics (wettability). During the evaporation of the solvent, a subtle balance between solution flow and adsorption of molecular aggregates can be expected. If both processes are out of sequence during the evaporation stage, less well-defined rings result which lack internal order. This was observed in the case of rings formed on untreated glass (Table 1). It should be noted that at low relative humidity (RH ~40–45%), no rings are formed. It is feasible that during the substrate- and sample preparation, water molecules from the atmosphere are physisorbed on the surface and that the properties of the layer of adsorbed water molecules depend on the relative humidity of the surrounding air. Possibly, the wettability of the carbon-coated substrates is influenced by the coverage of the surface with water molecules. We are currently investigating this effect in more detail.

As far as the molecular properties are concerned, the molecular aggregates need to be sufficiently soluble to prevent precipitation and consequent adsorption to the surface at a too early stage. Hexamers **2** and **1b** were found to aggregate at a slightly lower concentration than **1a**.[47] In the case of **1b** this can be ascribed to the enhanced intermolecular interactions due to the metal centers. However, the lower solubility of hexamers **2** is probably due to the chiral, branched tails that are shorter than the hexadecoxytails of **1** and thereby less capable to solubilize the aromatic porphyrin cores. In this study it was observed that rings formed by **1b** are quite comparable to those formed by **1a**, as could be expected from the similarity of the molecules. The only significant difference is revealed when the degree of fluorescence anisotropy is evaluated for rings formed by **1a** as compared to rings of **2**. The chiral hexamer **2** forms small rings with pronounced polarization effects on both hydrophobic and hydrophilic carbon-coated surfaces, whereas **1a** forms polarized rings only on hydrophophilic carbon-coated glass (Table 1). Furthermore, the measurement of the fluorescence anisotropy throughout the rings confirmed quantitatively that molecules of the chiral hexamer **2** are better ordered within the rings than those of **1a**. It is reasonable to assume that because of the chiral, branched tails, the molecules of **2** are less flexible to fit into columnar stacks. Therefore, during the aggregation of **2** in solution the molecules will rearrange until they are optimally organized in the columnar stacks, which eventually adsorb to the surface. In other words, we propose that the ordering within the ring is determined to a large extent by the intermolecular aggregation processes in solution during the formation of the rings.

On carbon-coated glass surfaces better-defined rings are formed than on untreated glass (Table 1). Especially on a hydrophilic carbon-coated glass surface, rings of either **1a** or **2** are not only more monodisperse in size but also much smaller. This appears to relate to the observed polarization effect, since surprisingly, only small rings (5 μm or smaller) displayed fluorescence anisotropy, indicative of a high degree of internal order. Previous studies have reported that additional treatment of the rings such as annealing could provide the molecules with sufficient energy to rearrange into the right orientation *after* formation of the rings.[41] It is interesting to note that in the present study, most of the small rings are already polarized and no additional annealing is needed.

It is clear that only small rings are ordered internally and all large rings are not ordered. Nevertheless, not all small rings are ordered. This observation suggests that whether a ring is ordered or not is not simply determined by thermodynamics but that other processes play a role. It can be explained by the way in which the (small) rings are formed, that is, via heterogeneous nucleation of holes or via spinodal dewetting. The first way of dewetting would lead to unordered rings that are randomly distributed and can have different ring sizes; the resulting rings can be small by coincidence. The latter way of dewetting takes place at a later stage when the solution is already concentrated and intermolecular aggregation processes have already taken place. Therefore, the columnar stacks that are aligned via spinodal dewetting would be more organized before they are deposited around the pinhole as depicted in Figure 8d. The resulting rings would all have similar sizes which would be smaller on an average and possess a high degree of internal order. The hydrophilic carbon-coated glass appears to promote the spinodal dewetting to take place and suppress dewetting via heterogeneous nucleation, while on the hydrophobic carbon-coated surfaces more heterogeneously formed rings are observed. Spinodal dewetting is generally reported to occur on homogeneous surfaces. This implies that the hydrophilic carbon-coated surface is more homogeneous than the hydrophobic carbon-coated glass substrate. The hydrophilic carbon coating which is applied on top of the hydrophobic carbon-coated glass is assumed to be very thin (only a few nm thick) and is therefore not expected to be able to make the surface more homogeneous in a topological way, but it may very well be able to make it chemically more homogeneous.

Conclusion

We have shown that we are able to construct well-defined, circular porphyrin architectures with a high degree of internal order on a molecular level. The porphyrin rings are readily formed on several substrates by depositing a solution droplet on a surface and allowing the solvent to evaporate. Since there is no material in the interior of the rings, they must be formed according to a pinhole mechanism rather than via a coffee-stain mechanism. During the ring-formation process, two tandem processes of dewetting and self-assembly of the molecules in solution take place simultaneously. The porphyrin hexamer molecules self-assemble into columnar stacks while in a tandem precipitation process, the aggregates are aligned radially around the pinhole. The size and shape of the resulting rings and their internal ordering depend heavily on several parameters, namely wettability of the surface and solubility, stackability and adsorption properties of the molecules. By balancing these parameters, we can construct rings with control over dimensions and inter-

nal ordering. A hydrophilic carbon coating on glass substrates has proven to be the best suitable surface to fabricate small, very well-defined rings that are relatively monodisperse in size (1–4 μm) and display a high degree of fluorescence anisotropy. The investigation of the polarized fluorescence microscopy images has enabled us to derive the precise orientation of the molecules and to quantify the degree of order of the molecules within the rings.

Since we can design and construct rings with desired morphology and internal molecular order we intend to make rings composed of different porphyrin derivatives, such as porphyrins containing catalytic transition metals. We are currently developing these rings as heterogeneous catalysts by using manganese porphyrin hexamers. In addition, concerning the orientation of the molecules within the rings, we will study energy transfer from the interior of the rings to the outside and vice versa and apply these ring-shaped architectures in molecular electronics.

Experimental Section

Synthesis: Compound **1** was synthesized according to a literature procedure.[14] The chiral hexamer **2** was synthesized in an analogues fashion from the chiral tail substituted benzaldehyde. Full details concerning the synthesis of **2** will be described elsewhere.

Surface preparation: In order to assess the ring-forming capability of the molecules and to determine ring sizes and shapes the ring samples were first prepared on carbon-coated copper grids and studied by transmission electron microscopy (TEM). However, for fluorescence microscopy these substrates are not sufficiently flat. To prepare flat hydrophobic substrates, round cover glasses (diameter 10 mm) were coated with a carbon film. The cover glasses were first rinsed with boiling ethanol and blow-dried with a heat gun and were subsequently put in an Edwards 306 apparatus. The carbon film was created in vacuum by putting an electric current (three times during 3 s) through carbon electrodes consisting of chalk coal pencils placed 20 cm above the cover glasses. The carbon is presumably deposited as an amorphous layer (~100 nm thick) on the glass substrates. The hydrophilic carbon-coated surfaces were made by depositing a second carbon film containing electrostatic charges on top of the hydrophobic carbon-coated cover glasses. The carbon-coated cover glasses were placed on a round electrode (10 cm in diameter) in a Balzers BSV apparatus. The chamber was evacuated and at reduced pressure, benzene vapor was led in. The carbon-coating was then applied by putting an electric current over the electrodes (10 cm apart), thereby discharging the benzene vapor. The benzene fragments are deposited on the substrates to form a thin hydrophilic carbon layer (estimated thickness ~4 nm).

Sample preparation: The samples were prepared by depositing 3 μL droplets of 2 μM solutions of **1** and **2** in chloroform on a substrate and allowing the solvent to evaporate completely (during about 10 s) under ambient conditions.

Fluorescence microscopy and spatially resolved fluorescence spectra: The output of an Argon ion laser (460 or 514 nm) was focused on the sample by a 50× microscope objective to a 50 μm diameter spot. The polarization of the excitation laser beam could be changed without affecting the excitation volume, by using a combination of a Glan–Taylor polarizer and a Babinet–Soleil compensator. The fluorescence from the sample was collected by the same objective and guided through a dichroic mirror and a long-pass filter, in order to eliminate the laser light reflected by the sample. In the fluorescence microscope measurements, the fluorescence was directly imaged on a nitrogen cooled, back illuminated CCD camera (Princeton Instruments, 512×512 pixels) through a Glan–Taylor polarizer. In the spatially and spectrally resolved fluorescence measurements, the fluorescence was imaged on the entrance slit (slit width: 200 μm) of an imaging monochromator (HR 640, Jobin-Yvon) through a polarizer and recorded by a nitrogen cooled, back illuminated CCD camera (Princeton Instruments, 1300×100 pixels). The picture recorded by the CCD camera is spectrally and spatially resolved along its orthogonal axes, with resolutions of 0,1 nm and ~1 μm, respectively.

Absorption spectra: The absorption spectra of solutions and rings on glass substrates were measured by a single grating spectrometer and a linear diode array (Ocean Optics). A halogen lamp and a deuterium lamp coupled into an optical fiber were used for excitation.

Atomic force microscopy: The atomic force microscopy image was recorded using a Digital Instruments AFM equipped with a Nanoscope IIIa controller (DI) in the tapping mode at room temperature in air.

Acknowledgement

The authors wish to thank Prof. F. C. de Schryver and Prof. J. Hofkens for many fruitful discussions and help in setting up this research project and F. J. P. Wijnen for assistance with the AFM measurements. In addition, NRSC-Catalysis and the Stichting voor Fundamenteel Onderzoek (FOM) financially supported by NWO are acknowledged for financing.

[1] S. Scheuring, J. Seguin, S. Marco, D. Levy, B. Robert, J. L. Rigaud, *Proc. Natl. Acad. Sci. USA* **2003**, *100*, 1690–1693.
[2] G. McDermott, S. M. Prince, A. A. Freer, A. M. Hawthornthwaite-lawless, M. Z. Papiz, R. J. Cogdell, N. W. Isaacs, *Nature* **1995**, *374*, 517–521.
[3] T. J. Meyer, *Acc. Chem. Res.* **1989**, *22*, 163–170.
[4] I. S. Choi, N. Bowden, G. M. Whitesides, *Angew. Chem.* **1999**, *111*, 3265–3268; *Angew. Chem. Int. Ed.* **1999**, *38*, 3078–3081.
[5] C. M. Drain, *Proc. Natl. Acad. Sci. USA* **2002**, *99*, 5178–5182.
[6] J.-M. Lehn, *Supramolecular Chemistry*, Wiley-VCH, Weinheim, **1995**.
[7] S. Hecht, *Angew. Chem.* **2003**, *115*, 24–26; *Angew. Chem. Int. Ed.* **2003**, *42*, 24–26.
[8] J. A. A. W. Elemans, A. E. Rowan, R. J. M. Nolte, *J. Mater. Chem.* **2003**, *13*, 2661–2670.
[9] J.-M. Lehn, *Science* **2002**, *295*, 2400–2403.
[10] W. I. White, *The Porphyrins, Vol. 5*, Academic Press, New York, Chapter 7, **1978**.
[11] P. J. Thomas, N. Berovic, P. Laitenberger, R. E. Palmer, N. Bampos, J. K. M. Sanders, *Chem. Phys. Lett.* **1998**, *294*, 229–232.
[12] E. Umbach, K. Glockler, M. Sokolowski, *Surf. Sci.* **1998**, *404*, 20–31.
[13] S. Yoshimoto, A. Tada, K. Suto, R. Narita, K. Itaya, *Langmuir* **2003**, *19*, 672–677.
[14] H. A. M. Biemans, A. E. Rowan, A. Verhoeven, P. Vanoppen, L. Latterini, J. Foekema, A. P. H. J. Schenning, E. W. Meijer, F. C. de-Schryver, R. J. M. Nolte, *J. Am. Chem. Soc.* **1998**, *120*, 11054–11060.
[15] J. Foekema, A. P. H. J. Schenning, D. M. Vriezema, F. B. G. Benneker, K. Norgaard, J. K. M. Kroon, T. Bjørnholm, M. C. Feiters, A. E. Rowan, R. J. M. Nolte, *J. Phys. Org. Chem.* **2001**, *14*, 501–512.
[16] Y. U. Cai, S. L. Bernasek, *J. Am. Chem. Soc.* **2003**, *125*, 1655–1659.
[17] J. A. A. W. Elemans, M. C. Lensen, J. W. Gerritsen, H. van Kempen, S. Speller, R. J. M. Nolte, A. E. Rowan, R. J. M. Nolte, *Adv. Mater.*, in press.
[18] C. A. Hunter, J. K. M. Sanders, *J. Am. Chem. Soc.* **1990**, *112*, 5525–5534.
[19] I. Yin, Q. Guo, R. E. Palmer, N. Bampos, J. K. M. Sanders, *J. Phys. Chem. B* **2003**, *107*, 209–216.
[20] A. P. H. J. Schenning, F. B. G. Benneker, H. P. M. Geurts, X. Y. Liu, R. J. M. Nolte, *J. Am. Chem. Soc.* **1996**, *118*, 8549–8552.
[21] L. Latterini, R. Blossey, J. Hofkens, P. Vanoppen, F. C. de Schryver, A. E. Rowan, R. J. M. Nolte, *Langmuir* **1999**, *15*, 3582–3588.
[22] L. D. Qin, H. B. Li, L. X. Wu, D. L. Qiu, X. Zhang, J. C. Shen, *Chem. Lett.* **2003**, *32*, 390–391.
[23] U. Thiele, M. Mertig, W. Pompe, *Phys. Rev. Lett.* **1998**, *80*, 2869–2872.
[24] K. Shafi, I. Felner, Y. Mastai, A. Gedanken, *J. Phys. Chem. B* **1999**, *103*, 3358–3360.

[25] V. F. Puntes, K. M. Krishnan, A. P. Alivisatos, *Science* **2001**, *291*, 2115 – 2117.
[26] S. L. Tripp, S. V. Pusztay, A. E. Ribbe, A. Wei, *J. Am. Chem. Soc.* **2002**, *124*, 7914 – 7915.
[27] T. Vossmeyer, S. W. Chung, W. M. Gelbart, J. R. Heath, *Adv. Mater.* **1998**, *10*, 351 – 353.
[28] P. C. Ohara, J. R. Heath, W. M. Gelbart, *Angew. Chem.* **1997**, *109*, 1123 – 1125; *Angew. Chem. Int. Ed. Engl.* **1997**, *36*, 1078 – 1083.
[29] R. D. Deegan, O. Bakajin, T. F. Dupont, G. Huber, S. R. Nagel, T. A. Witten, *Nature* **1997**, *389*, 827 – 829.
[30] R. D. Deegan, O. Bakajin, T. F. Dupont, G. Huber, S. R. Nagel, T. A. Witten, *Phys. Rev. E* **2000**, *62*, 756 – 765.
[31] P. C. Ohara, W. M. Gelbart, *Langmuir* **1998**, *14*, 3418 – 3424.
[32] A. Martin, A. Buguin, F. Brochard-Wyart, *Langmuir* **2001**, *17*, 6553 – 6559.
[33] H. Hu, R. G. Larson, *J. Phys. Chem. B* **2002**, *106*, 1334 – 1344.
[34] G. Reiter, *Phys. Rev. Lett.* **1992**, *68*, 75 – 78.
[35] S. Herminghaus, K. Jacobs, K. Mecke, J. Bischof, A. Fery, M. Ibn-Elhaj, S. Schlagowski, *Science* **1998**, *282*, 916 – 919.
[36] M. Mertig, U. Thiele, J. Bradt, D. Klemm, W. Pompe, *Appl. Phys. A: Mater. Sci. Process* **1998**, *66*, 565-568.
[37] K. Kargupta, R. Konnur, A. Sharma, *Langmuir* **2001**, *17*, 1294 – 1305.
[38] A. Sharma, R. Khanna, *Phys. Rev. Lett.* **1998**, *81*, 3463 – 3466.
[39] U. Thiele, K. Neuffer, Y. Pomeau, M. G. Velarde, *Colloids Surf. A* **2002**, *206*, 135 – 155.
[40] S. de Feyter, J. Hofkens, M. Van der Auweraer, R. J. M. Nolte, K. Müllen, F. C. de Schryver, *Chem. Commun.* **2001**, 585 – 592.
[41] J. Hofkens, L. Latterini, P. Vanoppen, H. Faes, K. Jeuris, S. de Feyter, J. Kerimo, P. F. Barbara, F. C. de Schryver, A. E. Rowan, R. J. M. Nolte, *J. Phys. Chem. B* **1997**, *101*, 10588 – 10598.
[42] F. Balzer, J. Beermann, S. I. Bozhevolnyi, A. C. Simonsen, H.-G. Rubahn, *Nano Lett.* **2003**, *3*, 1311 – 1314.
[43] J. M. Ribo, J. M. Bofill, J. Crusats, R. Rubires, *Chem. Eur. J.* **2001**, *7*, 2733 – 2737.
[44] H. S. Cho, D. H. Jeong, S. Cho, D. Kim, Y. Matsuzaki, K. Tanaka, A. Tsuda, A. Osuka, *J. Am. Chem. Soc.* **2002**, *124*, 14642 – 14654.
[45] Unpublished results.
[46] A. M. Higgins, R. A. L. Jones, *Nature* **2000**, *404*, 476 – 478.
[47] Critical aggregation constants were determined by the onset of fluorescence quenching at 3.0×10^{-6} M, 5.4×10^{-7} M and 5.7×10^{-7} M for **1a**, **1b** and **2**, respectively.

Received: August 9, 2003 [F5436]

